ELSEVIER

Polymer 42 (2001) 8987–8998

polymer

www.elsevier.com/locate/polymer

Diffusion and aggregation of hydrogeneous and deuterated polyethylene chains at their interfacial boundary as studied by time- and space-resolved FTIR microscopic measurements

Kohji Tashiro*, Naomi Gose

Department of Macromolecular Science, Graduate School of Science, Osaka University, 1-1 Machikaneyama-cho, Toyonaka, Osaka 560-0043, Japan

Received 22 February 2001; received in revised form 17 April 2001; accepted 17 April 2001

Abstract

In order to clarify the origins of cocrystallization and phase segregation phenomena observed for blend samples between fully-deuterated high-density polyethylene (DHDPE) and hydrogeneous linear low-density polyethylene (LLDPE) with various degrees of ethyl branchings, diffusion process of deuterated (D) and hydrogeneous (D) polyethylene chains through the contact interface between the D and H films was traced in situ by time-resolved Fourier-transform infrared spectroscopic measurement at temperatures above the melting points, from which the diffusion coefficients were evaluated. Spatial distribution of D and H chains in the interfacial region of the contacted films was also observed at room temperature by infrared spectral measurement for the melt-quenched samples: the homogeneous mixing was observed for a pair of DHDPE and LLDPE(2) with 17 ethyl branchings per 1000 carbon atoms and the heterogeneous distribution for a pair of DHDPE and LLDPE(3) with 41 ethyl branchings per 1000 carbon atoms. From the spatial distribution data the diffusion coefficients were evaluated again, consistent with that obtained by the time-resolved experiment. Activation energy for the diffusion motion of chains was also estimated from the temperature dependence of the diffusion coefficient. A large difference in diffusion coefficient and activation energy was found between the above-mentioned two sample systems, relating well with the difference in the aggregation state of D and H chains in the melt as well as in the crystallized sample: cocrystallization phenomenon for DHDPE/LLDPE(2) and phase segregation for DHDPE/LLDPE(3).

Keywords: Polyethylene; Cocrystallization; Phase segregation

1. Introduction

In order to understand the relationship between structure and properties of polymer blends, a clarification of aggregation state of different polymer species in the blend is basically important. A typical example is the blends of polyethylene (PE) with different degrees of side branching, which have been investigated for a long time from various points of view in order to clarify the aggregation state of the different components [1–43]. But, because of the similarity in chemical structure of the PE components, it is not easy to trace the behavior of the individual components separately.

As one of the useful techniques for this purpose, the utilization of deuterated species has been proposed. The blends between the hydrogeneous (H) and deuterated (D) PE species were investigated by means of vibrational spectroscopy and neutron scattering. In case of infrared spectroscopy the difference in vibrational frequency between the CH_2 and CD_2 groups can be utilized, making it possible to trace the behavior of each species separately [1–4,7,28,32–35,39,40,43–46]. Especially a Fourier-transform infrared spectrometer (FTIR) is particularly useful for this purpose because the H and D infrared bands can be detected simultaneously and separately. Krimm et al. showed that the splitting widths of the crystalline bands of methylene bending and rocking modes change sensitively depending on the aggregation state of the H and D chain stems in the crystalline lattice [1–4,7]. Neutron scattering technique is another useful method to trace the spatial distribution of the D and H chains in the PE blends, where the difference in the coherent scattering amplitude between the H and D species is utilized [47–60]. In this way the PE blends between the D and H species are useful for the study of aggregation state of PE chains, but there had been one serious problem in these studies. This was about the phase segregation between the D and H species. For a long time people had used the blends

* Corresponding author. Tel./fax: +81-6-6850-5455.
E-mail address: ktashiro@chem.sci.osaka-u.ac.jp (K. Tashiro).

0032-3861/01/$ - see front matter
PII: S0032-3861(01)00378-0

of the D and H species of high-density PE (HDPE) with no side chain branching. But, when these blend samples were cooled slowly from the molten state, the D and H chains were found to crystallize separately, i.e. the phase segregation phenomenon occurred [44,47–50]. Therefore, the H/D blend samples had to be prepared by quenching from the molten state to avoid the phase segregation between these two species. That is to say, the study of PE blends between D and H species had been limited to the samples prepared in a special manner. This was a dilemma for the study of chain aggregation structure in the samples crystallized under the normal conditions.

In a series of papers, Tashiro et al. reported that the blend samples of deuterated high-density PE (DHDPE) and hydrogeneous linear low-density PE (LLDPE) with a certain degree of side chain branchings show almost perfect cocrystallization phenomenon and both the components coexist in the same crystalline lamella *even when they are cooled slowly from the melt* [28,29,32–35,38–40,43]. Aggregation structure of chains and crystallization behavior were investigated from the molecular level by means of wide-angle and small-angle X-ray scatterings (using a synchrotron radiation), infrared spectra, differential scanning calorimetry, small-angle light scattering, neutron scattering, and so on. The crystallization behavior was found to depend on the degree of branching of the H species. For example, in case of the blend between DHDPE and LLDPE(2) with 17 ethyl branchings per 1000 carbon atoms, almost perfect cocrystallization is observed, while for the blend between DHDPE and LLDPE(3) with ca. 41 ethyl branchings the sample segregates into the two phases of the H and D species when the sample is crystallized by slow cooling from the melt. The blend between DHDPE and HDPE without any side group exhibits also the phase segregation. Neutron scattering experiments showed that the H and D chains are homogeneously mixed in the molten state for all of the above-mentioned pairs of D and H species.

In what mechanism do the segregation and cocrystallization occur from the homogeneously mixed molten state? For example, it might be reasonable to speculate that the D and H chains in the melt experience the diffusional motion at different rates and the chains of similar species gather to crystallize into their own lamellae, resulting in the phase segregation. In the case of cocrystallization phenomenon, the D and H chains diffuse at almost the same rate in the melt and are stabilized into the state of coexistence in the same lamella. In this way, both kinetic and thermodynamic factors need to be considered when a formation mechanism is discussed about the aggregation structure of the different species [40]. As for the thermodynamic factor, the analysis about the DSC data observed for the cocrystallized DHDPE/LLDPE(2) blend samples was already made: the D/H blend content dependence of the melting temperature could be simulated reasonably [43]. As another important factor for the phenomena of cocrystallization and segregation, we need to study the kinetic problem, i.e. the diffusion of D and H chains in the melt. In other words, we need to clarify the interpenetration behavior of the H and D chains in the molten state.

Such a study about the diffusion of H and D chains in the melt is important also from the industrial point of view. For example, two kinds of pipes, each of which is made of a different kind of PE, are connected to each other to be used as a hybrid water pipe [61,62]. The strength of the connection part of these two pipes is determined by the degree of cocrystallization of the two kinds of PE used for these pipes. Therefore, interpenetration of different kinds of PE chain at the interfacial part of these two pipes must be clarified in relation with the formation process of the aggregation structure of different kinds of PE chains in the vicinity of the connection part.

In the present paper, we will investigate the diffusion of H- and D-PE chains in the molten states in order to understand the aggregation process of these two kinds of PE chains to form the crystalline lamellae. More concretely speaking, the H- and D-PE samples were connected and the interpenetration process of D and H chains was observed by measuring the change in the relative content of the H and D chains at the interfacial part of these connected samples as functions of time and position. The diffusion process was traced in situ by carrying out the time-resolved measurement of FTIR spectra at various temperatures above the melting points by means of an infrared microscope. From the thus obtained experimental data, the mutual diffusion coefficients were evaluated by analyzing the concentration profile of the D and H chains as a function of time. In situ measurement of FTIR spectra in the process of interpenetration of H- and D-PE chains may be the first trial as long as we know in the references. As another type of experiment, the band profile of infrared spectra was analyzed at the various positions of the H/D interface, where the spectra were measured at room temperature for the samples quenched after being kept for a while in the molten state. The band profile reflects quite sensitively the aggregation structure of the H and D chains. At the same time, an analysis was made for the concentration profile in the vicinity of the interfacial part, giving us an information about the diffusion process of the H and D chains in the molten state. After the completion of our experiments, we came to know that our investigation of spatial distribution of the H and D chains in the melt-quenched sample was not the first trial but was already reported by Klein et al. [63,64] for a pair of HDPE and DHDPE, although they evaluated only the concentration distribution at the interfacial part but did not analyze the spectral profile to clarify the aggregation structure of the H and D chains. As for the evaluation of diffusion coefficient of PE, there have been reports of studies by NMR method [65–68] and by a technique of microlayer melting temperature convergence [69], but the infrared spectroscopic method seems apt in that the concrete and local aggregation state of H and D chains can be searched in detail, as will be described in this paper.

Table 1
Characterization of PE samples used in the present study

	M_w	M_n	Ethyl branching/ 1000C	Melting point (°C)
DHDPE	107k	34k	2–3	116.0
LLDPE(2)	75k	37k	17	102.0
LLDPE(3)	61k	20k	41	60.0

2. Experimental

2.1. Samples

DHDPE was purchased from Merck Chemicals. For the H-PE samples, LLDPEs with different degrees of ethyl branching were used, which was supplied by Exxon. These samples were the same as those used in the previous papers and the behavior of these samples was already known well [28,29,32–35,38–40,43]. The characterization of these samples is listed in Table 1. These samples were melted and pressed on a hot stage at ca. 160°C and then cooled slowly to the room temperature. The film thickness was 20 μm for the infrared measurement.

For the measurements of infrared spectra at the interfacial part, the contact of the two films must be made perfectly. The films were cut into pieces of ca. 1×1 mm^2 so that the edges of the films were as sharp as possible. The D- and H-PE films were connected at their edges carefully and tightly and were fixed by being sandwiched between a pair of KBr single crystals. These processes were done under an optical microscope to keep the perfect contact of the two films at the edges. The sample was set on a hot stage of the infrared microscope, as illustrated in Fig. 1.

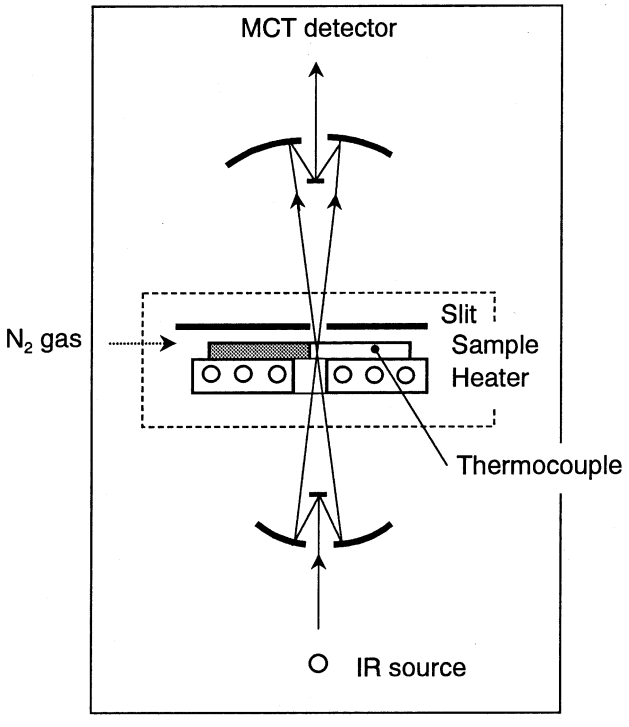

Fig. 1. An illustration of infrared microscopic measurement of diffusion process in the contacted DHDPE and LLDPE films. The infrared beam was focused on the interfacial part covered with thin slit of 39 μm width. The heater stage could be moved horizontally by using a micrometer.

For the experiment about the spatial distribution of the D and H chains in the boundary region, the connected films were heated above the melting points for a predetermined time, followed by quenching into liquid nitrogen to freeze the aggregation state of the melt.

2.2. Measurements

Fig. 2 shows the sample and the area for infrared measurement. In this study, two types of measurements were made. One was an in situ infrared measurement of the contact films at the boundary part shown in Fig. 2(a). The slit width of the microscope was 39 μm. The time-resolved measurement was made at an interval of ca. 40 s at a resolution power of 4 cm^{-1}. The sample was heated above the melting points of the D and H films (Table 1). In order to avoid the oxidation of the sample, nitrogen gas was made to flow around the sample. Another type of measurement was made at room temperature for the sample in contact, which had been heated above the melting points for a suitable time and quenched into liquid nitrogen to fix the spatial distribution of the D and H chains in the molten state. The infrared spectra were measured at the various parts of the sample by using a slit width of 8 μm at the resolution power of 2 cm^{-1}. The sample position was moved on a stage equipped with a micrometer. All the measurements of infrared spectra were made by using a Japan Spectroscopic Company FTIR microscope 'Janssen' equipped with an MCT (mercury cadmium telluride) detector.

3. Results and discussion

3.1. DHDPE/LLDPE(2) samples

3.1.1. Time-resolved measurements

A pair of DHDPE and LLDPE(2) shows the cocrystallization phenomenon when the blend sample was cooled slowly from the melt. In Fig. 3 is shown the time dependence of FTIR spectra in the frequency regions of CH_2 and CD_2 scissoring modes ($\delta(CH_2)$ and $\delta(CD_2)$, respectively), which were measured at the positions close to the contact interface between the D and H films at 133°C. When the observation was made at the H film side of the boundary, the infrared bands of the molten H species decreased in intensity with time, and at the same time the intensity of the D bands increased in intensity in parallel. The reverse phenomenon was observed at the boundary of the D film side: the D bands decreased in intensity and the H bands increased instead. Fig. 4 shows these situations more clearly, where the relative intensities of the $\delta(CH_2)$ and

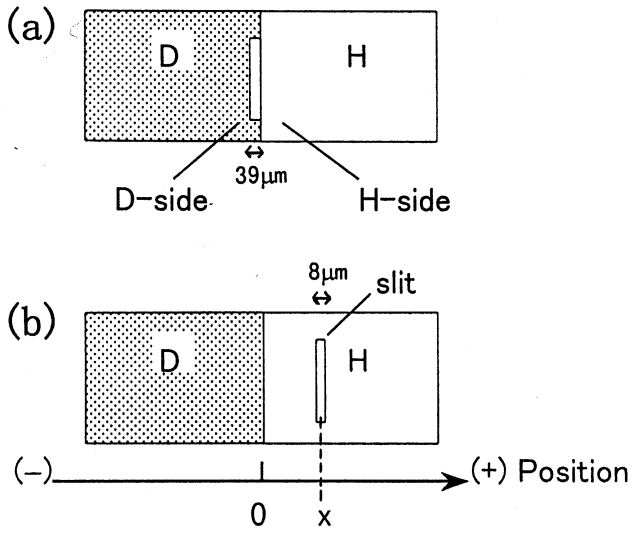

Fig. 2. Schematic illustration of the sample used for (a) time-resolved measurement and (b) space-resolved measurement.

$\delta(CD_2)$ bands were plotted against time, which were evaluated from the date of Fig. 3 by integrating the areas enclosed by base lines drawn from 1480 to 1420 cm^{-1} for $\delta(CH_2)$ and from 1150 to 1060 cm^{-1} for $\delta(CD_2)$. In this way, the mutual diffusion of the H and D chains into the

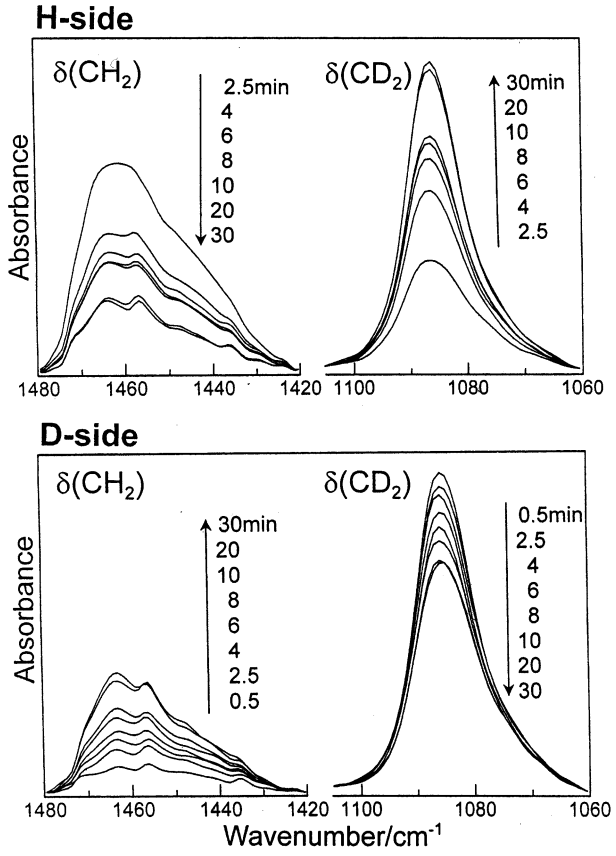

Fig. 3. Time dependence of infrared spectra in the regions of CH_2 and CD_2 scissoring modes measured for the molten sample at 133°C: (upper) H-side and (lower) D-side (refer to in Fig. 2).

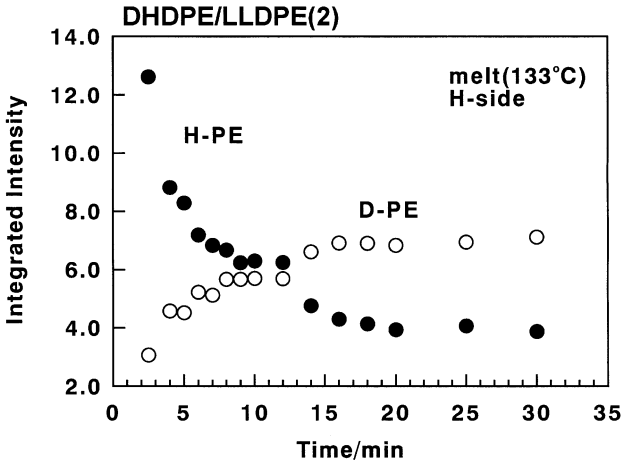

Fig. 4. Time dependence of integrated intensities of $\delta(CH_2)$ and $\delta(CD_2)$ bands measured in the H film side of contacted films (refer to Figs. 2 and 3).

D and H film sides, respectively, could be observed directly by carrying out the time-resolved FTIR measurements.

The relative content of the D and H chains in the interfacial region can be estimated as a function of time in the following way. Integrated intensity of the D and H bands, $A(D)$ and $A(H)$, respectively, are expressed by the following equations on the basis of Lambert–Beer's law.

$$A(D) = \epsilon(D)c(D)d \quad (1)$$

$$A(H) = \epsilon(H)c(H)d \quad (2)$$

where $\epsilon(i)$ and $c(i)$ are, respectively, a molar extinction coefficient and a molar concentration of the component i (=D or H) and d is the film thickness. Since $c(D) + c(H) = 1$, then we have

$$A(D) = -[\epsilon(D)/\epsilon(H)]A(H) + \epsilon(D)d \quad (3)$$

Fig. 5 shows the plot of $A(D)$ vs. $A(H)$ made by using the data of Fig. 4. A straight line was obtained, from the slope of which the ratio $\epsilon(D)/\epsilon(H)$ could be evaluated as indicated in

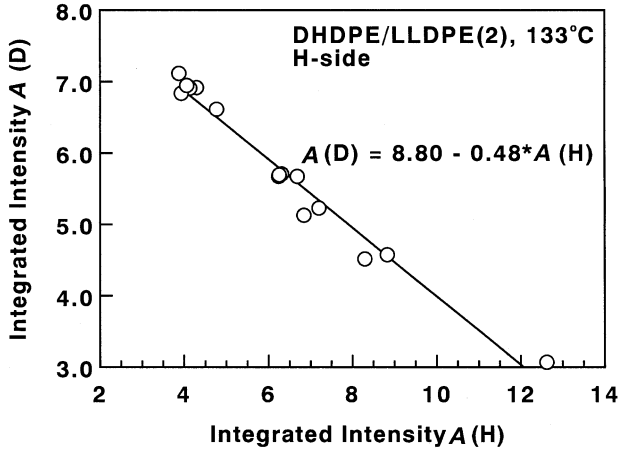

Fig. 5. Linear relation between integrated intensities $A(D)$ and $A(H)$ evaluated in Fig. 4.

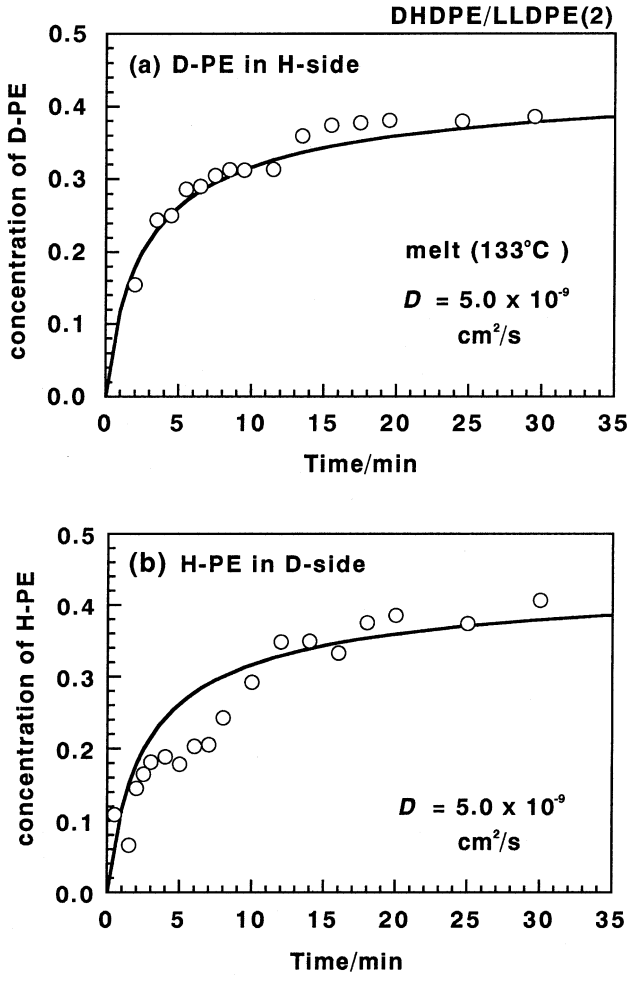

Fig. 6. Time dependence of relative concentrations evaluated from the data of Fig. 5: (a) for D species in the H side and (b) for H species in the D side. The solid lines represent the theoretical curves calculated from Eq. (6) in the text.

this figure. On the other hand, from Eqs. (1) and (2), the c(D) is expressed as follows.

$$c(\mathrm{D}) = \frac{A(\mathrm{D})/A(\mathrm{H})}{\epsilon(\mathrm{D})/\epsilon(\mathrm{H}) + A(\mathrm{D})/A(\mathrm{H})} \tag{4}$$

Therefore, by substituting the values of A(D) and A(H) into Eq. (4), the relative content of the D species can be evaluated as a function of time. Fig. 6(a) shows the thus obtained time dependence of c(D) at 133°C. Fig. 6(b) is the case of c(H), the relative content of the H chain species migrated into the D film side, where the data are a little more scattered than that of c(D) possibly due to some experimental problem.

Now, by using the curves shown in Fig. 6, the mutual diffusion coefficient D may be estimated on the basis of the Fickian diffusion. It is assumed here that no anomalous effect occurs for the diffusion of these polymers and that the D is independent of the concentration and the measurement position, and then

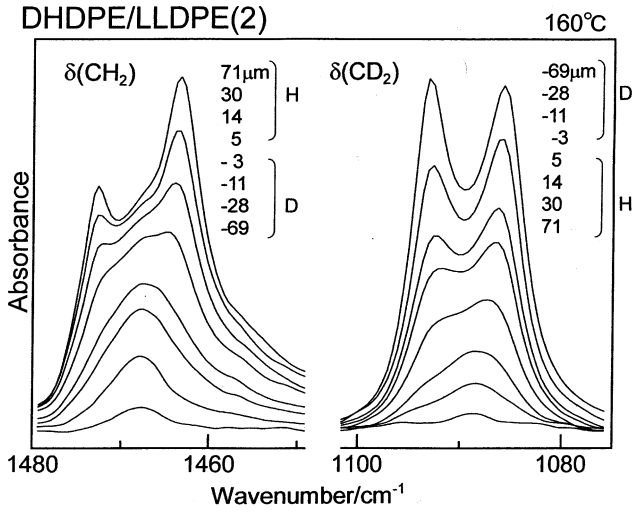

Fig. 7. Infrared spectra in the regions of CH_2 and CD_2 scissoring modes measured at various positions for a pair of contacted DHDPE and LLDPE(2) films quenched after being kept at 160°C for 10 min. The measured positions were indicated by figures with μm unit (refer to in Fig. 2).

$$\partial c/\partial t = D[\partial^2 c/\partial x^2] \tag{5}$$

where c is the concentration distribution of a particular species, x is the distance from the origin or the interface and t is a diffusion time in the molten state. For the system of two infinitely long plates connected at one edge, a solution for c can be given by the following equation [70].

$$c(x,t) = (1/2)c_0 \cdot \mathrm{erfc}[x/(2\sqrt{Dt})] \tag{6}$$

$$\mathrm{erfc}(z) = 1 - (2/\sqrt{\pi}) \int_0^z \exp(-y^2)\, \mathrm{d}y \tag{7}$$

where c_0 is the initial concentration at a boundary ($=1$). The theoretical curve given by Eq. (6) could reproduce the observed data of Fig. 6 by choosing a proper D value by a trial-and-error method, as indicated by solid curves in Fig. 6. The thus evaluated D coefficient is 5.0×10^{-9} cm^2/s for the mutual diffusion of D and H chains at 133°C.

Similar experiments were tried at different temperatures, but an oxidation of the sample proceeded seriously at higher temperature, as detected by an increasing intensity of C=O stretching band at 1750 cm^{-1}, even when nitrogen gas was made to flow in the sample box.

3.1.2. Spatial distribution and aggregation structure of D and H chains

The infrared spectra measured for the molten state cannot give us any details of the spatial distribution of the H and D chains in the boundary region of the contacted samples, although an information is obtained about the population of H and D chains at various positions. In order to know the spatial distribution of the H and D chains in more detail, the sample was kept for a predetermined time above the

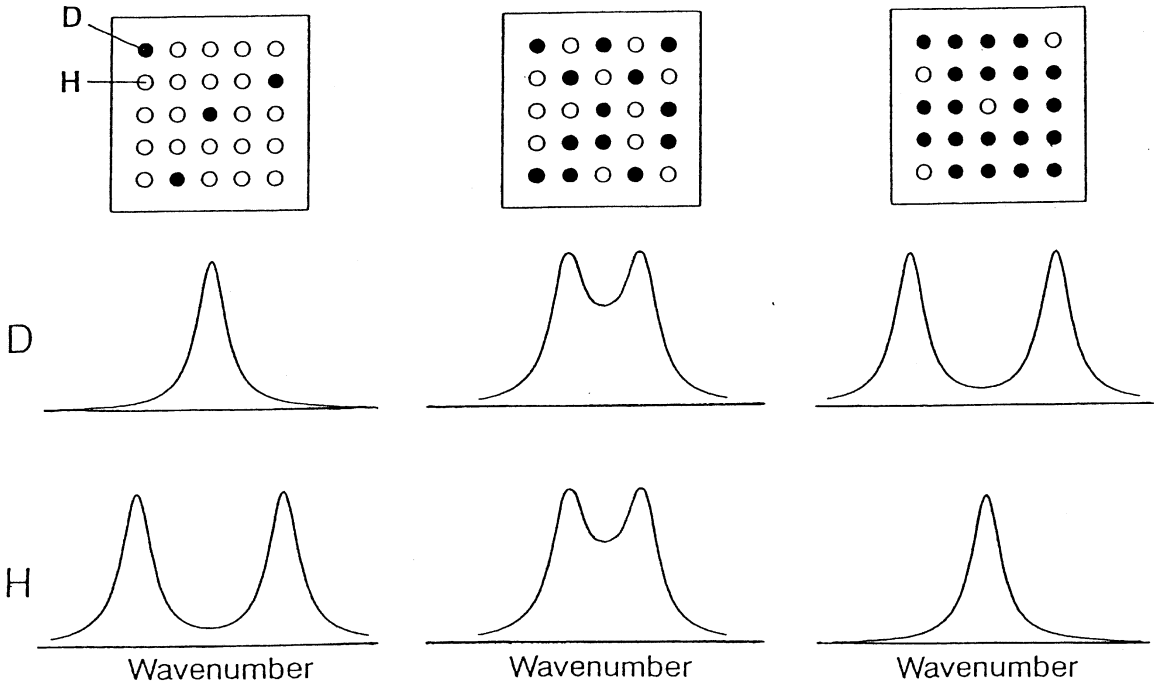

Fig. 8. Schematic illustration of the relation between molecular aggregation state and infrared spectral profile. Open and solid circles represent, respectively, the H and D chain stems in the crystal lattice. As the D chain stems are isolated by the H chain stems, the singlet component increases for the D band and the band splitting width becomes narrower.

melting point and was quenched into liquid nitrogen to freeze the aggregation state in the molten state. In spite of drastic quenching, the crystallization occurred very fast and the IR spectra of the crystalline state were obtained at room temperature. We assume here that the centers of mass of the chains in the melt do not change even after quenching and only the local regularization of the chain segments is allowed to occur to give the crystalline lamellae. This assumption is similar to the 'Ersterrungsmodell (solidification model)' proposed by Stamm et al. [56,58]. According to this model, the radius of gyration of a chain is kept even after the crystallization. In fact, the small-angle neutron scattering data supported it also for the present DHDPE/LLDPE(2) blend sample [43].

Fig. 7 shows the infrared spectra in the regions of $\delta(CH_2)$ and $\delta(CD_2)$ modes. The spectra were measured at room temperature at various positions in the vicinity of contact interface of the H and D films, which were quenched after being kept at 160°C for 10 min. Figures with μm unit indicate the position of the infrared measurement: the 0 position is just the interface and the plus and minus values correspond to the positions in the H and D film side, respectively, as illustrated in Fig. 2(b). The $\delta(CH_2)$ band is seen to decrease in intensity as the measurement position moves from the H to D side through the interfacial boundary. In contrast to it, the $\delta(CD_2)$ band decreases in intensity as the measurement position changes from the D to H side. A more important point is that the band profile changes depending on the measurement position. As already discussed in the previous papers [32–35,38–40], the profile of infrared bands of orthorhombic PE crystal changes depending on the aggregation state of the H and D chains, as illustrated in Fig. 8. For pure H (or D) sample, the $\delta(CH_2)$ [or $\delta(CD_2)$] splits into two due to the intermolecular vibrational coupling between the adjacent two chain stems arrayed along the (110) direction in the unit cell. If an H (D) chain is isolated from the surrounding H (D) chains by an invasion of the D (H) chains and the vibrational coupling between the adjacent H (or D) chains is cut, then the band profile changes into a singlet [1–4]. In this way, depending on the environmental atmosphere, the band profile changes continuously between doublet and singlet. In fact, the band profile measured for the DHDPE/LLDPE(2) blend samples with various D/H ratios changes continuously as shown in Fig. 9. The change in the band profile observed in Fig. 7 indicates an occurrence of similar phenomenon in the interfacial region of the H and D films. In the boundary of the H film side, the D chains migrate from the D film side and are mixed up with the originally-existing H chains and cocrystallize together when the sample is cooled to room temperature. Because the concentration of the D chains in the H film decreases gradually as the position is more distant from the interface, the $\delta(CD_2)$ band profile changes from doublet to singlet. As for the $\delta(CH_2)$ band, the situation is reverse and the band profile changes from doublet to singlet as the measurement position changes from the H side to the D side.

In this way the change in the band profile depends on the spatial arrangement of the D and H chains in the crystal

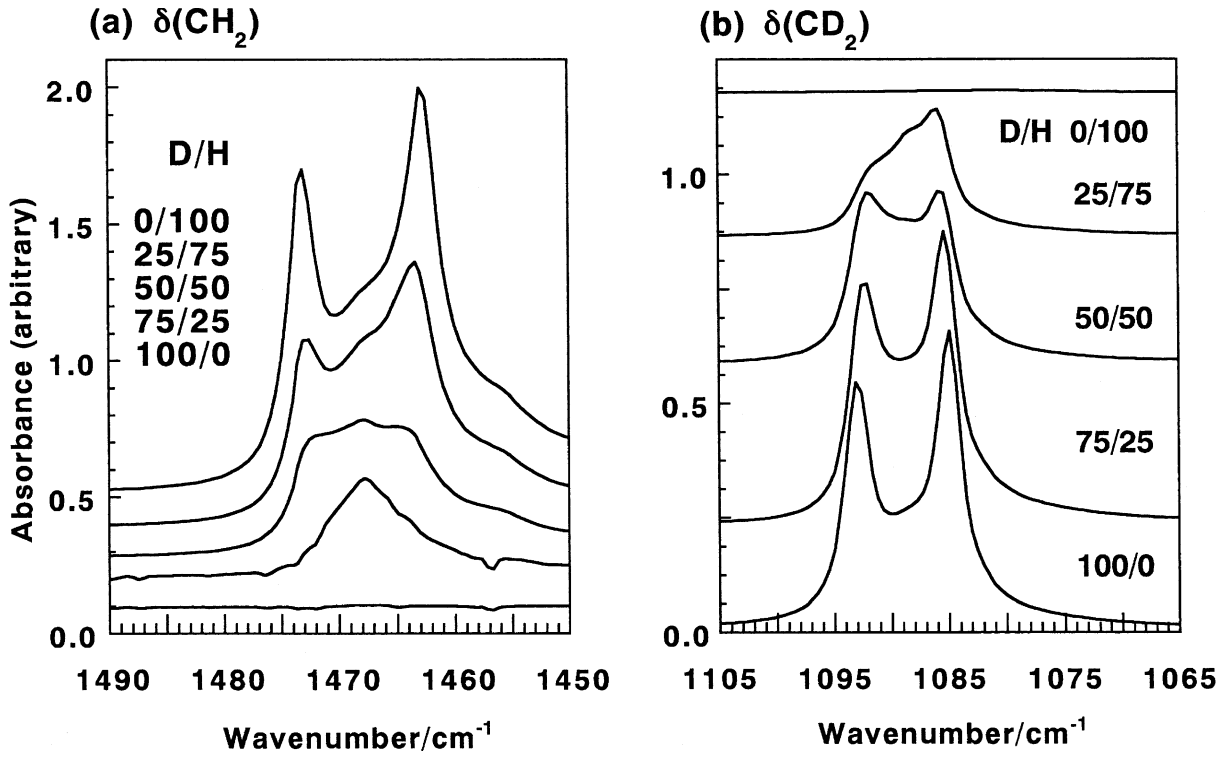

Fig. 9. Infrared spectra in the regions of CH_2 and CD_2 scissoring modes measured at room temperature for a series of DHDPE/LLDPE(2) blend samples. The resolution power of the spectra was 1 cm^{-1}.

lattice. Therefore, by analyzing the band profile, we may estimate the aggregation structure of the D and H chains in the crystal lattice more quantitatively. As reported in the previous papers [32–35], the band profile was separated into components of doublet and singlet. Originally, the band splitting width should change continuously and the band profile needs to be separated into infinite number of doublets and singlet, and so the unique answer is difficult to obtain. Therefore, in the present study, the doublet component was assumed to be only one, corresponding to the average of the doublets with various splitting widths [32–35]. Fig. 10 shows the thus analyzed results for the $\delta(CH_2)$ band profile. The intensity of doublet and singlet components changed continuously depending on the position of the measurement. The singlet component of the H band increased in intensity and simultaneously the band splitting width decreased gradually as the measurement position shifted from the H side to the D side. In the D side, on the other hand, the band intensity of the H chains decreased and the band profile became singlet as the position was distant from the boundary. The infrared band intensity of the singlet component shows a maximum at the boundary, since the relative content of the singlet increases in the D side but the absolute concentration of the H chain is lower.

At the starting point we intended to estimate the diffusion of the D and H chains and their spatial distribution in the molten state of the contacted D and H films. As long as we assume that the spatial distribution of the centers of mass of molten PE chains is frozen by quenching (or even by slow cooling) and only the small changes in the local conformations of chains result in the regularization of the whole system [43], the information obtained in Fig. 10 may be directly translated to the D/H chain distribution in the molten state. Fig. 11(a) shows the concrete spatial distribution of the D and H chains in the melt. As the contact time of the D and H films in the molten state increases, migration of these chains is more evolved, and the H (D) chains are dispersed into the D (H) film. The migrating H (D) chains are diluted gradually by the surrounding D (H) chains and the H (D) chains reached at a distance quite far from the boundary are isolated from each other. It must be noticed here that such a homogeneous mixing phenomenon of the H and D chains can be observed for the sample system of DHDPE and LLDPE(2), which shows the perfect cocrystallization under any condition. The result on the DHDPE/LLDPE(3) system will be discussed in a later section, where the H and D species cannot be diluted homogeneously but the phase segregation occurs between these two species.

3.1.3. Diffusion coefficient

At this stage where we know the details of the spatial distribution of the H and D species, the diffusion coefficient D can be evaluated on the basis of Eq. (6). Fig. 12 shows the distribution of D species in the interfacial part, which was evaluated by using Eq. (4) from the integrated intensities of

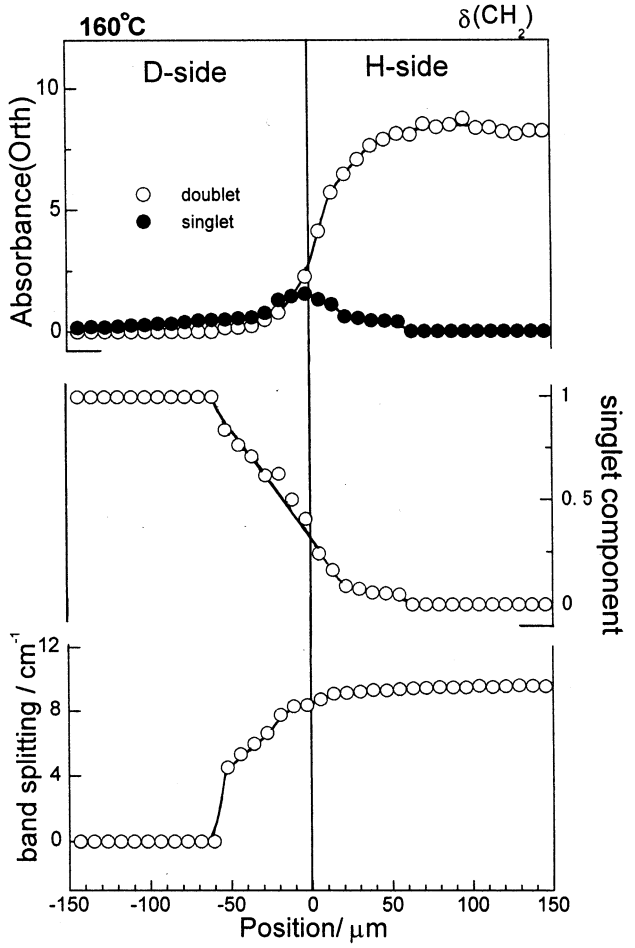

Fig. 10. Position dependence of (top) the relative intensity of doublet and singlet band components, (middle) the contribution of the singlet component, and (bottom) the splitting width of the doublet band component evaluated for the CH_2 scissoring band of the contacted DHDPE and LLDPE(2) films, which were quenched from 160°C after being kept for 10 min.

$\delta(CH_2)$ and $\delta(CD_2)$ bands. Similar to the case of time-dependent c(D) curve (Fig. 6), the D coefficient was estimated by fitting the curve of Fig. 12 to the theoretical one. The obtained D coefficient was 5.8×10^{-9} cm^2/s for the sample melted at 137°C for 10 min. Similar analysis was made for the samples treated at various temperatures and the obtained D coefficients are listed in Table 2. The D values are in relatively good coincidence with those reported in the references when the molecular weights of the samples are taken into account [64–69].

The thus-obtained D value was found to change with temperature where the samples were melted. As being usually made, this temperature dependence can be expressed by an Arrhenius type of equation.

$$D = D_0 \exp(-E_a/RT) \quad (8)$$

where E_a is an activation energy of diffusion, R is a gas constant and D_0 is a constant. By plotting $\ln D$ against $1/T$, E_a can be evaluated as a slope of the straight line, as shown in Fig. 13, where the D value evaluated from the time-dependence of c(D) is also included. The E_a for a pair of DHDPE and LLDPE(2) is 19.9 kJ/mol, which is in good agreement with the values 21–28 kJ/mol reported for HDPE [66,68,69].

3.2. DHDPE/LLDPE(3) samples

3.2.1. Segregation of D and H chains

When DHDPE and LLDPE(3) are blended together and cooled slowly from the melt, the segregation phenomenon is observed between the D and H lamellae, different from the case of DHDPE/LLDPE(2) system. Fig. 14 shows a series of FT-IR spectra in the $\delta(CH_2)$ and $\delta(CD_2)$ regions measured at room temperature for the contacted D/H samples which were heated at 160°C for 10 min followed by quenching into liquid nitrogen temperature. Since the degree of crystallinity is low for LLDPE(3), the splitting of $\delta(CH_2)$ band is difficult to detect, while the $\delta(CD_2)$ band shows clear splitting and does not change its profile at any position, very different from the case of DHDPE/LLDPE(2) system. Fig. 15 compares the position dependence of the splitting width of $\delta(CD_2)$ band between DHDPE/LLDPE(2) and DHDPE/LLDPE(3) systems. For DHDPE/LLDPE(2) system, the band splitting width changes continuously depending on the position and no difference is detected for the behavior between the two different temperatures of 129 and 180°C. On the other hand, for DHDPE/LLDPE(3) system, the band splitting width of $\delta(CD_2)$ changes slightly in the interfacial region of the H side but does not change perfectly to singlet profile even when the D chains migrate deeply into inner-side of the H film. This tendency was seen more clearly for the case at 133°C. Therefore, main conclusion obtained from these experimental data about the DHDPE/LLDPE(3) system is that the D and H chains migrate to mix in the molten state but they show a kind of microscopic segregation *when viewed from the scale detected by infrared spectroscopy* and they form segregated crystalline domains consisting of pure D or H species when crystallization is induced by quenching. Quite slight change in band splitting width, as observed in the spectra measured at room temperature, means an occurrence of local coexistence of DHDPE and LLDPE(3) chains in the interfacial region in a small scale. This is consistent with the observation reported in the previous papers [32–35].

On the basis of these experimental data about the

Table 2
Diffusion coefficients D evaluated at various temperatures

Temperature (°C)	DHDPE/LLDPE(2)	DHDPE/LLDPE(3)
129	4.6×10^{-9} cm^2/s	–
133	5.0[a]	1.5×10^{-9} cm^2/s
137	5.8	–
160	7.5	4.0
180	9.2	–

[a] Evaluated from the data of time-dependence of relative concentration (see Fig. 6).

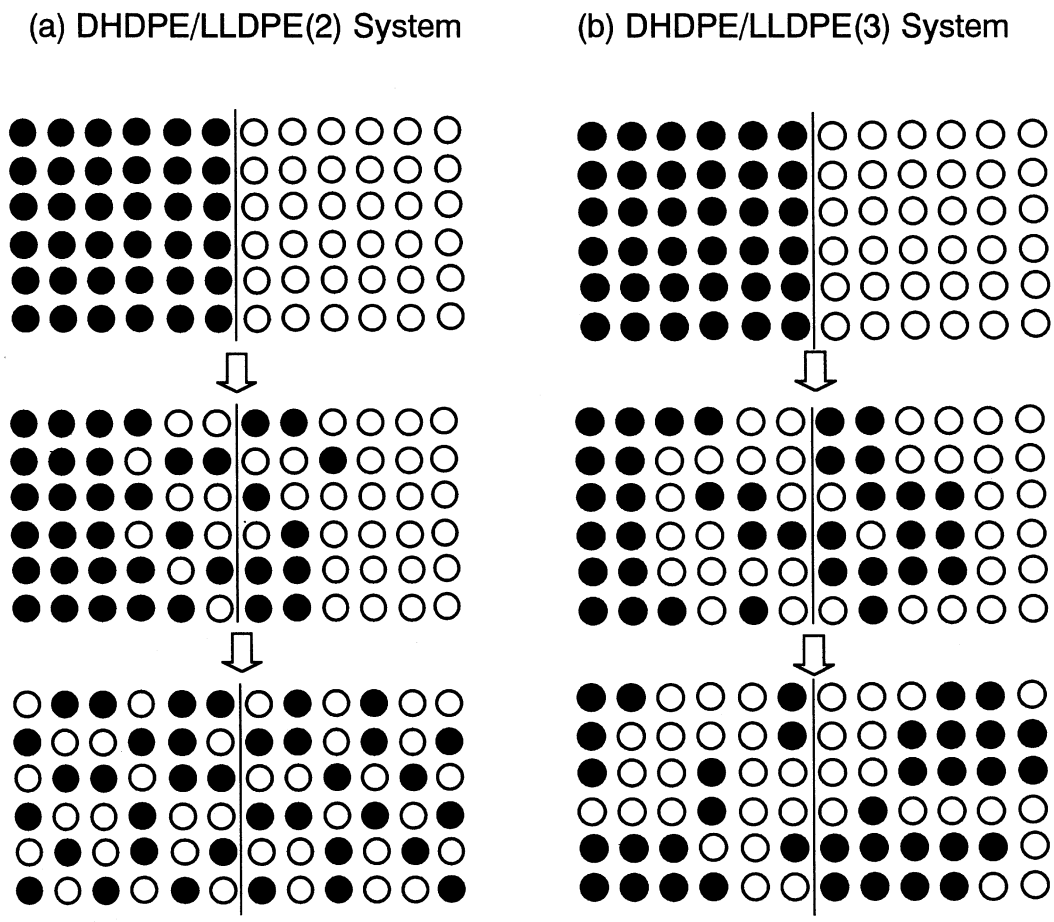

Fig. 11. Illustration of diffusion process of D (solid circles) and H (open circles) chains passing through the interface between the D and H films: (a) the case of DHDPE/LLDPE(2) system and (b) the case of DHDPE/LLDPE(3) system.

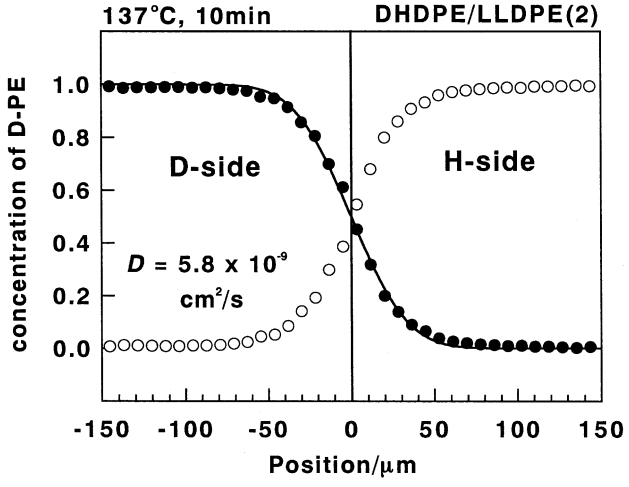

Fig. 12. Position dependence of the relative concentration of D (solid circles) and H (open circles) species for the contacted DHDPE and LLDPE(2) films, which were quenched from 137°C after being kept for 10 min.

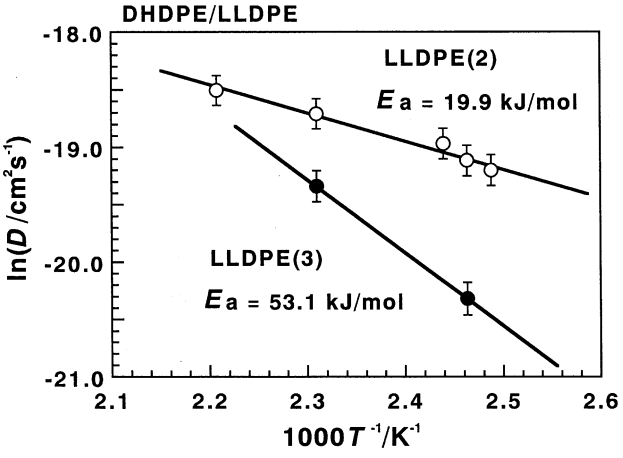

Fig. 13. Plot of logarithm of diffusion coefficient D against an inversed temperature made for (open circles) DHDPE/LLDPE(2) pair and (solid circles) DHDPE/LLDPE(3) pair. E_a is the activation energy for the mutual diffusion motion.

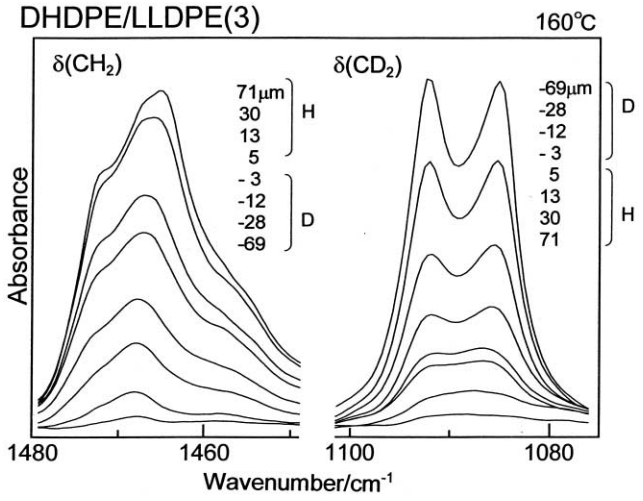

Fig. 14. Infrared spectra in the regions of CH_2 and CD_2 scissoring modes measured at various positions for a pair of contacted DHDPE and LLDPE(3) films quenched after being kept at 160°C for 10 min. The measured positions were indicated by figures with μm unit (refer to in Fig. 2).

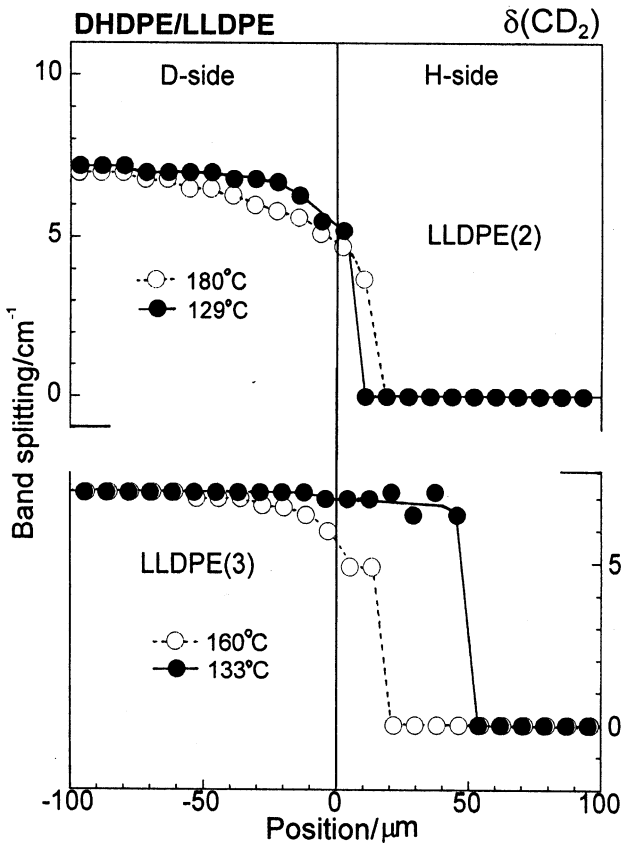

Fig. 15. Position dependence of band splitting width evaluated for the CD_2 scissoring band for (upper) the contacted DHDPE/LLDPE(2) films which were quenched after being kept at 180 and 129°C for 10 min and (lower) the connected DHDPE/LLDPE(3) films quenched from 160 and 133°C after 10 min.

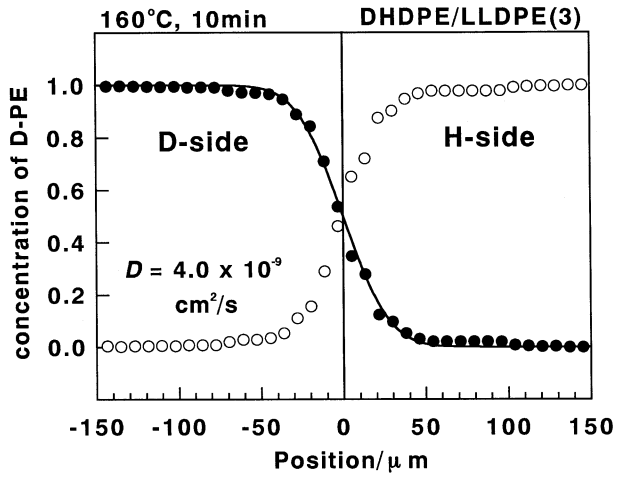

Fig. 16. Position dependence of the relative concentration of D (solid circles) and H (open circles) species for the contacted DHDPE and LLDPE(3) films, which were quenched from 160°C after being kept for 10 min.

aggregation structure of the D and H chain components, the diffusion of these chains in the melt at the interfacial part may be drawn illustratively as shown in Fig. 11(b). In the case of DHDPE/LLDPE(2), the D and H components migrate into the regions of the other components homogeneously and are gradually diluted at deeper positions of the films. For DHDPE/LLDPE(3), diffusion occurs with keeping coagguration of D (or H) chains and the partial mixing of the D and H components occurs in limited parts. In the previous papers we measured the small-angle neutron scatterings (SANS) for the molten DHDPE/LLDPE(3) blend samples and indicated a homogeneous mixing of the D and H chain components [38,43] but, the present infrared spectral data showed the segregation of individual components in the molten state. This might be a contradiction between these two experimental data. This apparent contradiction is considered to come from the difference in the scale viewed by SANS and FTIR spectroscopy. In the scale of several tens nanometers or from the view of neutron scattering the D and H chains are seen to mix homogeneously in the melt. But, the infrared spectra showed us a local structure of much smaller scale. As shown in Fig. 11, in the case of DHDPE/LLDPE(3) system, the microscopic segregation of H and D domains is considered to occur when viewed from the infrared spectroscopy but it is viewed to be rather homogeneous from SANS eye.

3.2.2. Diffusion coefficients

By integrating the total areas of the $\delta(CH_2)$ and $\delta(CD_2)$ bands, concentration distribution of H and D chains were evaluated in a similar way to that described in the previous section. Fig. 16 shows the spatial distribution of relative concentration of D species for the sample treated at 160°C for 10 min. The solid curve is the calculated result on the

basis of Eq. (6), and the D coefficient was evaluated as $D = 4.0 \times 10^{-9}$ cm^2/s. This value is smaller than the D value (7.5×10^{-9} cm^2/s) of DHDPE/LLDPE(2) system at almost the same temperature, indicating higher difficulty of the diffusion of the chains through the interface between DHDPE and LLDPE(3) films. In Table 2 are listed the D coefficients evaluated for DHDPE/LLDPE(3) samples at the different temperatures. Fig. 13 includes the Arrhenius plot for DHDPE/LLDPE(3) sample also. The activation energy was evaluated to be 53.1 kJ/mol, about 2.7 times higher than that of DHDPE/LLDPE(2). In this way, for the system of DHDPE/LLDPE(3), the diffusion coefficient is smaller and the activation energy of diffusion is higher, reflecting a strong tendency of segregation between the D and H chains, quite contrast to a strong tendency of mutual mixing of the D and H chains in the DHDPE/LLDPE(2) system.

4. Conclusions

In the present paper the time-resolved infrared measurement was made for the first time in the vicinity of the interfacial region of the connected D and H films by using an FTIR microscope. At the same time, the spatial distribution of the D and H chains was also investigated by measuring the infrared spectra at the various positions of the samples quenched from the molten state. From these data, the time dependence and spatial dependence of the relative concentration of D and H species could be evaluated reasonably and the mutual diffusion coefficients were estimated as a function of temperature on the basis of Fick's second law of diffusion.

As discussed repeatedly, a large difference between DHDPE/LLDPE(2) and DHDPE/LLDPE(3) exists in the phenomenon of cocrystallization and phase segregation of the D and H chain components when they are cooled from the melt. The present infrared spectral study clarified the homogeneous mixing of D and H chains for the DHDPE/LLDPE(2) system in the molten state, while the heterogeneous separation of D and H chains was observed for the DHDPE/LLDPE(3) system even in the molten state. From the SANS data, a homogeneous mixing was speculated for the latter system but maybe in a much wider scale than the local structure viewed by infrared spectroscopy. Based on these data, concrete image of diffusion of the D and H chains in the molten state could be drawn reasonably (Fig. 11). A large difference between DHDPE/LLDPE(2) and DHDPE/LLDPE(3) systems in the diffusion behavior and spatial distribution of the D and H chain components means a remarkable difference in the kinetic and thermodynamic behaviors, which reflects on the difference in the crystallization behavior between these two systems. It must be noticed that small differences in the degree of side branching between LLDPE(2) and LLDPE(3) results in large difference in diffusion and crystallization behaviors.

References

[1] Tasumi M, Krimm S. J Chem Phys 1967;46:755.
[2] Tasumi M, Krimm S. J Polym Sci, Part A-2 1968;6:995.
[3] Bank MI, Krimm S. J Polym Sci, Polym Phys Ed 1969;7:1785.
[4] Bank MI, Krimm S. J Polym Sci, Polym Lett Ed 1970;8:143.
[5] Stehling FC, Ergos E, Mandelkern L. Macromolecules 1971;4:672.
[6] Bukingham AD, Hentschel HGE. J Polym Sci, Polym Phys Ed 1980;18:853.
[7] Cheam TC, Krimm S. J Polym Sci, Polym Phys Ed 1981;19:423.
[8] Norton DR, Keller A. J Mater Sci 1984;19:447.
[9] English AD, Smith P, Axelson DE. Polymer 1985;26:1523.
[10] Hu S, Kyu T, Stein RS. J Polym Sci, Part B: Polym Phys 1987;25:71.
[11] Kyu T, Hu S, Stein RS. J Polym Sci, Part B: Polym Phys 1987;25:89.
[12] Ree M, Kyu T, Stein RS. J Polym Sci, Part B: Polym Phys 1987;25:105.
[13] Vadhar P, Kyu T. Polym Engng Sci 1987;27:202.
[14] Marand HL, Stein RS, Stack GM. J Polym Sci, Part B: Polym Phys 1988;26:1361.
[15] Alamo RG, Glaser RH, Mandelkern L. J Polym Sci, Polym Phys Ed 1988;26:2169.
[16] Rego Lopetz JM, Gedde UW. Polymer 1988;29:1037.
[17] Rego Lopetz JM, Conde Brana MT, Tersekius B, Gedde UW. Polymer 1988;29:1045.
[18] Hosoda S, Gotoh Y. Polym J 1988;20:17.
[19] Song HH, Stein RS, Wu DQ, Ree M, Philips JC, Legrand A, Chu B. Macromolecules 1988;21:1180.
[20] Rego Lopez JM, Gedde UW. Polymer 1989;30:22.
[21] Song HH, Wu DQ, Chu B, Satkowski M, Ree M, Stein RS, Philips JC. Macromolecules 1990;23:2380.
[22] Hill MJ, Barham PJ, Keller A, Rosney CCA. Polymer 1991;32:1384.
[23] Hill MJ, Barham PJ, Keller A. Polymer 1992;33:2530.
[24] Hill MJ, Barham PJ. Polymer 1992;33:4099.
[25] Jinnai H, Hasegawa H, Hshimoto T. Macromolecules 1992;25:6078.
[26] Iragorri JI, Rego JM, Katime I, Conde Brana MT, Gedde UW. Polymer 1992;33:461.
[27] Mandelkern L, McLaughlin KW, Alamo RG. Macromolecules 1992;25:1440.
[28] Tashiro K, Stein RS, Hsu SL. Macromolecules 1992;25:1801.
[29] Tashiro K, Satkowski MM, Stein RS, Li Y, Chu B, Hsu SL. Macromolecules 1992;25:1809.
[30] Graessley WW, Krishnamoorti R, Balsara NP, Fetters L, Lohse DJ, Schulz DN, Sissano JA. Macromolecules 1993;26:1137.
[31] Rhee J, Crist B. J Chem Phys 1993;98:4174.
[32] Tashiro K, Izuchi M, Kobayashi M, Stein RS. Macromolecules 1994;27:1221.
[33] Tashiro K, Izuchi M, Kobayashi M, Stein RS. Macromolecules 1994;27:1228.
[34] Tashiro K, Izuchi M, Kobayashi M, Stein RS. Macromolecules 1994;27:1234.
[35] Tashiro K, Izuchi M, Kaneuchi F, Jin C, Kobayashi M, Stein RS. Macromolecules 1994;27:1240.
[36] Alamo RG, Londono JD, Mandelkern L, Stehling FC, Wignall GD. Macromolecules 1994;27:411.
[37] Puig CC, Odell JA, Hill MJ, Barham PJ, Folkes MJ. Polymer 1994;35:2452.
[38] Tashiro K, Imanishi K, Izumi Y, Kobayashi M, Kobayashi K, Satoh M, Stein RS. Macromolecules 1995;28:8477.
[39] Tashiro K, Imanishi K, Izuchi M, Kobayashi M, Itoh Y, Imai M, Yamaguchi Y, Ohashi M, Stein RS. Macromolecules 1995;28:8484.
[40] Tashiro K. Acta Polym 1995;46:100.
[41] Stein RS, Cronauer J, Zachmann HG. J Mol Struct 1996;383:19.
[42] Schipp C, Hill MJ, Barham PJ, Cloke VM, Higgins JS, Oiarzabal L. Polymer 1996;37:2291.
[43] Sasaki S, Tashiro K, Gose N, Imanishi K, Izuchi M, Kobayashi M, Imai M, Ohashi M, Yamaguchi Y, Ohyama K. Polym J 677;31:1999.

[44] Spells SJ, Sadler DM. Polymer 1984;25:739.
[45] Spells SJ, Keller A, Sadler DM. Polymer 1984;25:749.
[46] Okoroafor EU, Spells SJ. Polymer 1994;35:4578.
[47] Stehling FC, Engos E, Mandelkern L. Macromolecules 1971;4:672.
[48] Ballard DGH, Wignall GD, Schelten J. Eur Polym J 1973;9:965.
[49] Kirste RG, Kruse WA, Schelten J. Makromol Chem 1973;162:299.
[50] Wignall GD, Ballard DGH, Schelten J. Eur Polym J 1974;10:801.
[51] Wunderlich B, Wignall GD, Ballard DGH, Shmatz W. Colloid Polym Sci 1974;252:749.
[52] Schelten J, Wignall GD, Ballard DGH. Polymer 1974;15:682.
[53] Schelten J, Ballard DGH, Wignall GD, Longman G, Schmatz W. Polymer 1976;17:751.
[54] Schelten J, Wignall GD, Ballard DGH, Longman GW. Polymer 1977;18:1111.
[55] Crystallization of polymers (special issue). Faraday Discuss Chem Soc 1979;68.
[56] Stamm M, Fischer EW, Dettenmaiere M, Convert P. Faraday Discuss Chem Soc 1979;68:263.
[57] Wignall GD, Mandelkern L, Edwards C, Glotin M. J Polym Sci, Phys Ed 1982;20:245.
[58] Stamm M. J Polym Sci, Phys Ed 1982;20:235.
[59] Londono JD, Narten AH, Wignall GD, Honnell KG, Hsieh ET, Johnson TW, Bates FS. Macromolecules 1994;27:2864.
[60] Alamo RG, Londono JD, Mandelkern L, Stehling FC, Wignall GD. Macromolecules 1994;27:411.
[61] Yoshida H, Tanaka A. Polym Prepr Jpn 1997;46:4031.
[62] Yoshida H, Yamauchi K, Maysui T, Tsuji K. Polym Prepr Jpn 1997;47:4175.
[63] Klein J. Nature 1978;271:143.
[64] Klein J, Briscoe BJ. Proc R Soc Lond A 1979;365:53.
[65] MaCall DW, Douglass DC, Anderson EW. J Chem Phys 1959;30:771.
[66] Fleischer G. Colloid Polym Sci 1987;265:89.
[67] Pearson DS, Ver Strate G, von Meerwall E, Schilling FC. Macromolecules 1987;20:1133.
[68] Bauchus R, Kimmich R. Polymer 1983;24:964.
[69] Schuman T, Stepanov EV, Nazarenko S, Capaccio G, Hiltner A, Bear E. Macromolecules 1998;31:4551.
[70] Crank J. Mathematics of diffusion. 2nd ed. London: Oxford University Press, 1975.